Contents lists available at ScienceDirect

Journal of CO2 Utilization

journal homepage: http://ees.elsevier.com

# Alternative carbon dioxide utilization in dimethyl carbonate synthesis and comparison with current technologies

J.D. Medrano-García *, J. Javaloyes-Antón, D. Vázquez, R. Ruiz-Femenia, J.A. Caballero

*Institute of Chemical Process Engineering, University of Alicante, PO 99E-03080, Alicante, Spain*

ARTICLE INFO

*Keywords*
$CO_2$ utilization
Dimethyl carbonate (DMC)
Methanol oxycarbonylation
Methane reforming
Superstructure decision making
Multi-objective optimization

ABSTRACT

Dimethyl carbonate (DMC) has recently gained popularity due to its environmentally friendly status and multiple applications in which it is able to replace more toxic chemicals. Among its several commercial synthesis production routes, the ethylene carbonate (EC) transesterification shines as a $CO_2$ consuming process. However, other factors such as the high emitting synthesis of EC precursors hinder its environmental capabilities. Methanol oxycarbonylation is a mature DMC non-$CO_2$ consuming synthesis route with the potential to indirectly utilize the greenhouse gas throughout the synthesis of its intermediates. In this work, we propose a DMC production superstructure using the methanol oxycarbonylation route with the aim of consuming $CO_2$ in both the synthesis gas (syngas) and methanol synthesis stages. Results show that the integration of methanol and syngas synthesis with the DMC production process vastly decreases both the cost and emission with respect to the unintegrated case. However, the addition of a Reverse Water Gas Shift (RWGS) reactor further decreases the emission down to a minimum of 1.019. kg $CO_2$-eq/kg DMC, resulting in a 54 % decrease in the indicator compared with the direct $CO_2$ utilization route. In comparison with other routes, utilization of this DMC in blends with gasoline manages to reduce the GWP of using the fuel mix to a potential 16 %.

**Nomenclature**

**Indices**

$c$
Cold stream: $C = \{(c)_{c=1}^{c=27}\}$

$cs$
Set relation between process section $s$ and cold stream $c$:

$$CS^{s,c} = \begin{cases} (SMR, c1), (SMR, c2), (POX, c3), (ATR, c4), (CR, c5), (CR, c6), \\ (DMR, c7), (DMR, c8), (BR, c9), (BR, c10), (TR, c11) \\ (RWGS1, c12), (RWGS1, c13), (RWGS2, c14), (RWGS2, c15), \\ (RWGS3, c16), (RWGS3, c17), (RWGS4, c18), (RWGS4, c19), \\ (MeOH, c20) \\ (DMC, c21), (DMC, c22), (DMC, c23), (DMC, c24), (DMC, c25), \\ (DMC, c26), (DMC, c27) \end{cases}$$

$comp$
Compressors in methanol synthesis: $COMP = \{(comp)_{comp=1}^{comp=5}\}$

$exit$
Exit in methanol synthesis process: $exit = \{feed, offgas\}$

$h$
Hot stream: $H = \{(h)_{h=1}^{h=25}\}$

$hs$
Set relation between process section $s$ and hot stream $h$:

$$HS^{s,h} = \begin{cases} (SMR, h1), (POX, h2), (ATR, h3), (CR, h4), (CR, h5), \\ (DMR, h6), (BR, h7), (TR, h8), (TR, h9), \\ (RWGS1, h10), (RWGS2, h11), (RWGS3, h12), (RWGS4, h13), \\ (MeOH, h14), (MeOH, h15), (MeOH, h16), (MeOH, h17), \\ (MeOH, h18), \\ (DMC, h19), (DMC, h20), (DMC, h21), (DMC, h22), (DMC, h23), \\ (DMC, h24), (DMC, h25) \end{cases}$$

$i$
Process units: $I = \{$syngas synthesis, flash separator, $CO_2$ absorber1, PSA $H_2$, cryogenic distillation, PSA CO, CO absorber, $CO_2$ absorber2, fuel cell, RWGS reactor$\}$

*Abbreviations*: CMO, Classic methanol oxycarbonylation; CCMO, $CO_2$-consuming methanol oxycarbonylation; DMC, Dimethyl carbonate; DME, Dimethyl ether; EC, Ethylene carbonate; EO, Ethylene oxide; GWP, Global warming potential; IMO, Integrated methanol oxycarbonylation; kg $CO_2$-eq, Kilograms of $CO_2$ equivalent; MO, Methanol oxycarbonylation; MTBE, Methyl tert buthyl ether; RWGS, Reverse water gas shift; STAC, Specific Total Annualized Cost.

* Corresponding author.
*E-mail address:* jd.medrano@ua.es (J.D. Medrano-García)

https://doi.org/10.1016/j.jcou.2021.101436
Received 14 September 2020; Received in revised form 21 December 2020; Accepted 4 January 2021
Available online xxx
2212-9820/

$j$
Components: $J =$ {methane, steam/water, $O_2$, $CO_2$, CO, $H_2$, MeOH, DMC}
$j'$
Component: $J' = \{j' \in J : j'$ is the reference component of process unit $i\} : \forall i \in I$
$k$
Unit types: $K =$ {reformer reactor, compressor, exchanger/heater/cooler, vessel, fuel cell}
$rwgs$
Reverse water gas shift reactor: $RWGS_i =$ {RWG1, RWG 2, RWG 3, RWG 4} : $i =$ {RWGS reactor}
$s$
Process sections: $S =$ {syngas synthesis, RWGS reactor, methanol synthesis, DMC production}
$st$
Heat integration stage: $ST = \left\{(st)_{st=1}^{st=69}\right\}$
$syn$
Syngas technologies: $SYN_i =$ {SMR, POX, ATR, CR, DMR, BR, TR} : $i =$ {syngas synthesis}
$u$
Utilities: $U =$ {natural gas, cooling water, electricity}

**Parameters**

$c_k^f$
Fixed cost parameter of unit type $k$ [$]
$c_k^v$
Variable cost parameter of unit type $k$ [$/capacity units]
$cost_{cold}$
Cold utility (cooling water) cost [$/kWh]
$cost_{elec}$
Electricity cost [$/kWh]
$cost_{hot}$
Hot utility (natural gas) cost [$/kWh]

$F_{j,0}^{MeOH,exit}$
Reference molar flows of component $j$ and exit $exit$ of methanol synthesis process [kmol/s]
$G_j$
Mole of $CO_2$ produced by the complete combustion per mole of component $j$ with air [kmol $CO_2$/kmol $j$]
$GWP_{elec}$
GWP indicator of electricity [kg $CO_2$-eq/kWh]
$GWP_{hot}$
GWP indicator of burning natural gas [kg $CO_2$-eq/kWh]
$IR$
Interest rate

$power_{comp,0}^{MeOH}$
Reference electricity consumption per compressor $comp$ in methanol synthesis [kW]
$years$
Horizon time [y]
$\Delta H_j^c$
Enthalpy of combustion of component $j$ [kJ/kmol $j$]
$\Delta T_{st}$
Temperature difference between stage $st$ and $st+1$

**Variables**

$cap_i$
Capital cost of process unit $i$ [$]
$cap^{MeOH}$
Capital cost of methanol synthesis [$]

$cost^{MeOH}$
Cost of methanol synthesis [$/s]

$cost^{util}$
Cost of hot and cold utilities [$/kWh]

$emission^{util}$
Emission associated to consuming hot utilities [kg $CO_2$-eq/kWh]

$emission^{MeOH}$
Emission of methanol synthesis [kg $CO_2$-eq/s]
$F_{DMC}$
Molar flow of product DMC [kmol/s]
$F_{j,in}^{DMC}$
Inlet molar flow of component $j$ in the DMC synthesis process [kmol/s]
$F_{j,offgas}^{DMC}$
Off-gas molar flow of component $j$ leaving the DMC synthesis process [kmol/s]
$F_{buy}^{MeOH}$
Molar flow of bought methanol [kmol/s]
$F_{j,in}^{MeOH}$
Inlet molar flow of component $j$ in the methanol synthesis process [kmol/s]
$F_{j,out}^{MeOH,s}$
Outlet molar flow of component $j$ of exit $s$ in the methanol synthesis process [kmol/s]
$F_j^{offgas}$
Molar flow of component $j$ in the off-gas [kmol/s]
$FCp_{stc}$
Product of the molar flow and heat capacity of cold stream $c$ in stage $st$ per kmol/h of component $j'$ [kW·ºC hkmol $j'$ ]
$FCp_{sth}$
Product of the molar flow and heat capacity of hot stream $h$ in stage $st$ per kmol/h of component $j'$ [kW·ºC hkmol $j'$ ]
$op^{MeOH}$
Operating cost of methanol synthesis [$/s]

$power^{DMC}$
Electricity consumption in DMC synthesis [kW]

$power^{MeOH}$
electricity consumption in methanol synthesis [kW]
$Q_{cold}$
Total cold services required by the system [kW]
$Q_i$
Hot services required by process unit $i$ [kW]
$Q_{hot}^{offgas}$
Hot services provided by fuel gas combustion [kW]
$Q_{hot}$
Total hot services required by the system [kW]
$R_{st}$
Residual heat that leaves stage $st$ [kW]

## 1. Introduction

Despite the efforts made by many countries, global carbon dioxide emissions have been growing annually, up to a 2.5 % in the last decade, without any sign of decrease. [1–3]. Since the shift towards renewable energy sources is not fast enough to palliate these emissions, Carbon Capture and Utilization (CCU) is seen as a complementary solution, not only to decrease them, but also to take advantage of the gas as a carbon source [4]. Among all the existing options that are being studied for CCU, dimethyl carbonate (DMC) is an environmentally friendly chemical with excellent solvent capabilities and applications in methylation and carbonylation reactions, as well as a precursor of polymers and in the energy sector [5–7]. In addition to its non-toxicity, its elevated oxygen content, higher than that of methyl tert butyl ether

(MTBE) and ethanol, make DMC a strong contestant for fuel additive in diesel and gasoline blends [5,8]. Moreover, DMC presents less $NO_x$ and soot emissions [9], and the increased efficiency achieved in the engine has been proved to further reduce both hydrocarbon and CO emissions in comparison with other oxygenated additives [10]. Industrially, DMC is mainly synthesized through carbonylation processes (over 90 % of global production [11]), being methanol oxycarbonylation, the preferred process of companies like Eni or Dow [5,6,12–14], the most prominent one.

Dimethyl carbonate has been recently flagged, along with methanol and methane, as one of the most interesting products from the $CO_2$-consumption perspective value [15]. As such, the valorization of $CO_2$ in the production of DMC has been extensively studied. Three main DMC synthesis technologies stand out as capable of consuming $CO_2$: direct synthesis with $CO_2$ and methanol, alcoholysis of urea, and transesterification of ethylene or propylene carbonate. The direct synthesis from $CO_2$, although apparently promising, presents thermodynamic limitations, such as low activation energy, deactivation of catalysts and reversibility of the reaction, that have prevented its industrial development [9,16]. The alcoholysis of urea, on the other hand, suffers from slow kinetics, low product selectivity and unfavorable thermodynamics [17]. Finally, the transesterification of ethylene or propylene carbonate is considered as a mature no-waste and renewable technology, that also produces ethylene/propylene glycol as a byproduct [17,18]. This route, especially the ethylene carbonate variant, has received plenty of interest from researchers, and is nowadays commercialized by Texaco, Shell and Asahi Kasei [13].

Nevertheless, in order to assess the environmental capabilities of a process, there are more factors to consider than just $CO_2$ utilization. Energy consumption and raw material usage play an important role in the net Global Warming Potential (GWP) of a process. This fact is proved by the study of Garcia-Herrero et al. [11], which consists in a Life Cycle Assessment (LCA) of the direct $CO_2$ and methanol process using an electrosynthesis reaction, resulting in a GWP indicator around 25 times higher than the one associated to the classic methanol oxycarbonylation process [11]. On the other hand, Kongpanna et al. [19] developed an LCA comparison study for several DMC routes. Their results show that the EC route achieves over a 10 % reduction in carbon emissions compared to the oxycarbonylation route, however, it misses to include raw materials as a source of indirect $CO_2$ emissions.

The transesterification of EC route requires ethylene oxide (EO), which has a production GWP of 2.1927 $kgCO_2$-eq/kg EO [20]. This synthesis is not only energy intensive, but also this chemical is hardly considered environmentally friendly [21]. Furthermore, EO synthesis produces $CO_2$ as a byproduct of the complete oxidation of ethylene [22]. As a consequence, the GWP of the EC route results in a value of 2.2347 $kgCO_2$-eq/kg DMC [20] even though $CO_2$ is consumed in the process. This fact raises the question of whether this technology is really worth it from a greenhouse gas abatement perspective.

The use of $CO_2$ as a precursor in the synthesis of carbon monoxide has been proven to drastically reduce the GWP indicator of the process, even surpassing the elusive carbon neutrality barrier [23]. Hence, CO derivatives, such as DMC from the methanol oxycarbonylation route, are likely to be affected by this decrease in emissions. For this reason, in this work, we propose a DMC production process integrating the syngas reforming (i.e. CO production), methanol synthesis and the methanol oxycarbonylation technology with the aim of getting a net $CO_2$ consumption. Since this process does not possess a direct $CO_2$ utilization reaction like the EC transesterification does, $CO_2$ consumption is accomplished in the methanol synthesis section and, especially, in the CO production stage.

To develop an optimal integrated process, we propose a superstructure (see Section 2) that considers all the alternatives of interest to generate and integrate syngas/CO synthesis with the methanol and methanol oxycarbonylation processes as well as a set of alternatives to adjust the $H_2$/CO ratio, increase the energy efficiency by using excess $H_2$ and separation/purification of CO needed in the oxycarbonylation section.

From the superstructure we develop a model using Generalized Disjunctive Programming (GDP) [24] and transforming the disjunctions into algebraic equations. A multi-objective MINLP model is solved using the epsilon constraint method [25], minimizing both the cost (Specific Total Annualized Cost, STAC) and the emission (GWP indicator) of the synthesis. The results provide the best structural configuration of the process and its optimal operating conditions.

As far as we know, this type of study on the methanol oxycarbonylation process has never been undertaken, since the direct $CO_2$ [26,27], urea [28–30] and ethylene carbonate routes [18] tend to take the spotlight in terms of $CO_2$ consumption in DMC synthesis. With this work, we intend to shed some light on an understudied process from the $CO_2$ utilization perspective, which has the potential to be on par with, or even surpass, other $CO_2$ consuming DMC production technologies. This reduced GWP in DMC production can potentially have a positive impact in its applications, both in the polymer industry, with increased $CO_2$-based polymers, and in the energy sector, cutting the emissions in current fuel blends.

## 2. Process and model description

The study of the DMC synthesis plant is carried out by performing multi-objective optimizations (simultaneous minimization of STAC and GWP) of an MINLP model. This model is based on a process superstructure containing several syngas synthesis and separation technologies as well as the full methanol synthesis loop (Fig. 1).

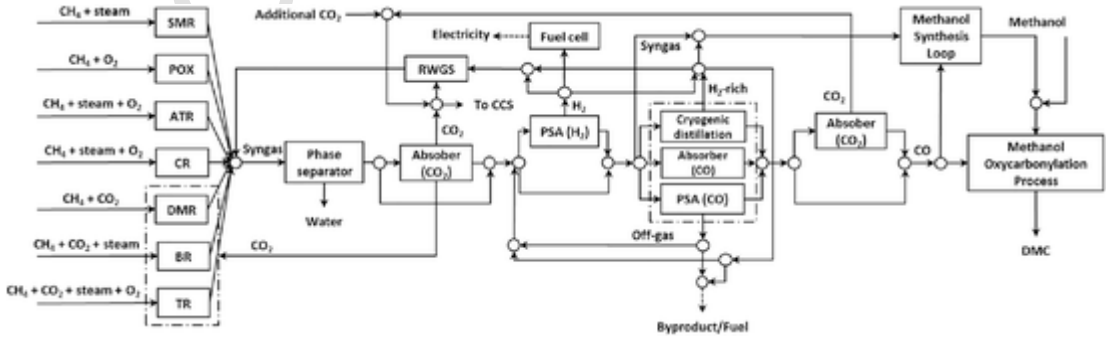


**Fig. 1.** Dimethyl carbonate (DMC) synthesis process superstructure. Steam Methane Reforming (SMR), Partial Oxidation (POX), Auto-thermal Reforming (ATR), Combined Reforming (CR), Dry Methane Reforming (DMR), Bi-reforming (BR) and Tri-reforming (TR), Reverse Water Gas Shift (RWGS), Pressure Swing Adsorption (PSA).

### 2.1. Synthesis gas and carbon monoxide production

First, syngas is obtained using one of seven different methane reforming technologies [31]: Steam Methane Reforming (SMR), Partial Oxidation (POX), Auto-thermal Reforming (ATR), Combined Reforming (CR), Dry Methane Reforming (DMR), Bi-reforming (BR) and Tri-reforming (TR). These processes are simulated in Aspen HYSYS using the most common available reaction data (Table 1):

The mixture then enters the composition adjustment stage, which includes a flash unit (phase separator) where all water is removed, an amine DGA (diglycolamine) based absorber [32] to remove $CO_2$, a pressure swing absorption (PSA) unit that targets $H_2$ and a number of CO purification processes such as cryogenic distillation, absorption with toluene and $CuAlCl_4$ and PSA unit. Alternatively, a syngas stream can be extracted right before this CO separation technology selection in order to act as a raw material for methanol production. Lastly, an additional $CO_2$ removal stage may be selected before CO is obtained. The off-gas resulting from the CO purification stage can be used as fuel within the system, valorized as a byproduct or recycled in order to take advantage of the unseparated $H_2$ and CO contained in it. The $H_2$ flow removed in the PSA unit can be used in a fuel cell in order to produce electricity or mixed with a $H_2$-rich stream, available if the cryogenic distillation process is selected, to be used as fuel, valorized as byproduct or enter the Reverse Water Gas Shift (RWGS) reactor, where it reacts with $CO_2$ extracted from the absorbers or, if necessary, even a stream from outside the process in order to produce additional CO. A comprehensive description of the syngas/carbon monoxide production section and a detailed mathematical model superstructure can be found in the supplementary material.

### 2.2. Methanol synthesis loop

Methanol is used as the second raw material in this DMC production pathway. Its synthesis is studied following the scheme shown in Fig. 2.

First, syngas enters the loop at 40 °C and 30 bar, which is then compressed and heated up to the reaction pressure and temperature. Kinetics [33] are considered for the following reactions:

$$CO + 2H_2 \rightleftarrows CH_3OH \quad (1)$$

$$CO_2 + 2H_2 \rightleftarrows CH_3OH + H_2O \quad (2)$$

**Table 1**
Reforming agent/methane molar ratio in the feed stream and operating conditions for each syngas process [31].

| | SMR | POX | ATR | CR | DMR | BR | TR |
|---|---|---|---|---|---|---|---|
| **$H_2O/CH_4$** | 3 | – | 1.43 | 2.5 | – | 1.6 | 2.46 |
| **$O_2/CH_4$** | – | 0.7 | 0.6 | 0.19 | – | – | 0.47 |
| **$CO_2/CH_4$** | – | – | – | – | 1 | 0.8 | 1.3 |
| **Temperature [°C]** | 900 | 800 | 750 | 850 | 850 | 850 | 827 |
| **Pressure [bar]** | 20 | 30 | 25 | 25 | 1 | 7 | 20 |

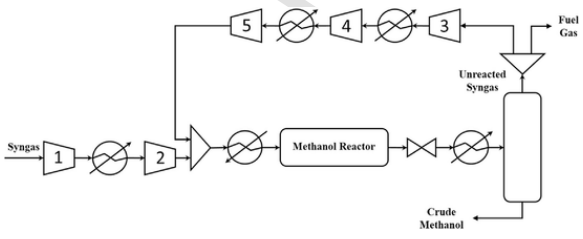


**Fig. 2.** Methanol synthesis loop.

$$CO + H_2O \rightleftarrows H_2 + CO_2 \quad (3)$$

After the reaction, the mixture is depressurized to 10 bar and split in a phase separator. Unreacted syngas is recompressed and recycled back to the reactor entrance, while crude methanol is obtained as a product. Reaction conditions and raw material composition are obtained from a series of optimizations varying syngas composition and reactor temperature and pressure, minimizing the cost per mass of product, which results are shown in Table 2. As a side note, syngas composition right at the entrance of the reactor has a $(H_2\text{-}CO_2)/(CO + CO_2)$ ratio of 2.04, which is the "slightly above 2.00 ratio" that is often talked about in methanol studies [34,35]. More details on the simulation and optimization study can be found in Medrano et al. (2017) [36].

The model for the methanol synthesis loop follows the minimum cost result of the optimization per kg of product [36]. According to the data shown in Table 2, inlet syngas composition is given by Eqs. (4) and (5):

$$0.05\left(F_{CO,in}^{MeOH} + F_{CO_2,in}^{MeOH}\right) = F_{CO_2,in}^{MeOH} \quad (4)$$

$$F_{H_2,in}^{MeOH} - F_{CO_2,in}^{MeOH} = 2.00\left(F_{CO,in}^{MeOH} + F_{CO_2,in}^{MeOH}\right) \quad (5)$$

where $F_{j,in}^{MeOH}$ stands for the inlet molar flow of component $j$ in the methanol synthesis section. These flows are supplied from a mixture of a split syngas flow removed immediately before the selection of the CO separation technology, an $H_2$-rich stream produced by cryogenic distillation (if selected), the off-gas produced as a byproduct of the general CO separation and a fraction of the separated CO. The outlet streams of this process comprise the product methanol, which is used as a raw material for the DMC synthesis, and an off-gas that is directly burnt as fuel or mixed with the off-gas obtained in the CO separation section. The off-gas composition stream is shown in Table 3.

Outlet streams of the methanol stage ($F_{j,out}^{MeOH,exit}$) are defined as follows (Eq. (6)):

$$F_{j,out}^{MeOH,exit} = \frac{F_{j,0}^{MeOH,exit} F_{CO,in}^{MeOH}}{F_{CO,0}^{MeOH,feed}} \quad \forall j, \forall exit \in [product, offgas] \quad (6)$$

Where $F_{j,0}^{MeOH,exit}$ represents the reference data showed in Table 3 and $F_{CO,0}^{MeOH,feed}$ is the reference molar flow of CO (0.285 kmol/s) that enters the synthesis loop. Any unreacted $CH_4$ from the syngas production stage that enters the loop is considered to exit in its totality with the off-gas.

**Table 2**
Methanol reactor conditions and raw material composition inlet into the loop.

| Molar syngas composition | | Reactor conditions | |
|---|---|---|---|
| **$(H_2\text{-}CO_2)/(CO + CO_2)$** | **$CO_2/(CO + CO_2)$** | **Temperature [°C]** | **Pressure [bar]** |
| 2.00 | 0.05 | 284.2 °C | 78.6 |

**Table 3**
Outlet stream molar flows (kmol/s) for a production of 789 t/d in the methanol synthesis loop.

| Component | $H_2$ | CO | $CO_2$ | $H_2O$ | MeOH |
|---|---|---|---|---|---|
| **Off-gas (kmol/s)** | $5.3\cdot10^{-2}$ | $1.8\cdot10^{-2}$ | $5.2\cdot10^{-3}$ | $3.9\cdot10^{-5}$ | $2.8\cdot10^{-3}$ |
| **Product (kmol/s)** | $0.1\cdot10^{-3}$ | $0.1\cdot10^{-3}$ | $1.2\cdot10^{-3}$ | $9.2\cdot10^{-3}$ | $2.7\cdot10^{-1}$ |

Hot and cold utility consumption is factored in along with the rest of the stages of the superstructure in Section 2.4, while electricity demand for the five compressors included in the methanol synthesis loop is shown in Table 4:

Electricity consumption ($power^{MeOH}$, kW) in the methanol production stage is calculated as (Eq. (7)):

$$power^{MeOH} = \sum_{comp \in [1,2,3,4,5]} \frac{power^{MeOH}_{comp,0} F^{MeOH}_{CO,in}}{F^{MeOH,feed}_{CO,0}} \quad \forall comp \tag{7}$$

where $power^{MeOH}_{comp,0}$ is the reference electricity demand for each compressor $comp$ (Table 4).

Alternatively, methanol can be directly bought from an external source with a price of 0.330 $/kg [30] and an associated production emission of 0.671 kg $CO_2$-eq/kg (Ecoinvent Database 3.5, Global market [37]). The cost ($cost^{MeOH}$, in $/s) of the methanol synthesis stage is calculated as follows (Eq. (8)):

$$cost^{MeOH} = cap^{MeOH} + op^{MeOH} + 0.330 F^{MeOH}_{buy} \tag{8}$$

where $F^{MeOH}_{buy}$ (kg/s) is the mass flow of methanol bought instead of produced, $cap^{MeOH}$ ($/s) is the annualized capital cost of the process units included in the synthesis loop (Eq. (9)) and $op^{MeOH}$ is the operating cost ($/s), which is calculated considering only electricity consumption (Eq. (10)), as other utilities are accounted for in the general heat integration of the system.

$$cap^{MeOH} = \left( \sum_k c^f_k + c^v_k A_k \right) \left( \frac{IR(IR+1)^{years}}{(IR+1)^{years} - 1} \right) \frac{1}{8000} \tag{9}$$

$$op^{MeOH} = power^{MeOH} cost_{elec} \tag{10}$$

Where the subscript $k$ represents the process units in the methanol synthesis loop (compressors, methanol reactor and phase separator), $c^f_k$ ($/s) and $c^v_k$ ($/(s·units)) are the fixed and variable cost parameters [31], *years* is the horizon time (8 years) and the interest rate ($IR$) is set to 0.1 [38], $A_k$ is the capacity of unit $k$ (consumed electricity for compressors (kW) and 100 $m^3$ for the vessel like units) and $cost_{elec}$ is the cost of using electricity (0.1305 kW [39]).

Associated emission of producing methanol ($emission^{MeOH}$, kg$CO_2$-eq/s) is again calculated from the consumption of electricity (assumed the European mix) and its GWP indicator ($GWP_{elec}$, 0.4473 kg$CO_2$-eq/kWh [39]) and any bought methanol in Eq. (11):

$$emission^{MeOH} = power^{MeOH} GWP_{elec} + 0.671 F^{MeOH}_{buy} \tag{11}$$

The energy produced by burning the off-gas, as well as its associated emission is included in the main off-gas valorization framework [23]. Further details on the the methanol synthesis stage are supported by the work of Medrano et al. (2017) [36].

**Table 4**
Electricity consumption for a production of 789 t/d in the methanol synthesis loop (Fig. 2).

| Compressor | 1 | 2 | 3 | 4 | 5 |
|---|---|---|---|---|---|
| Electricity demand [kW] | 1699 | 1722 | 4565 | 4791 | 5062 |

### 2.3. Dimethyl carbonate synthesis by methanol oxycarbonylation

The core of the superstructure is modelled after an Aspen Plus simulation of the methanol oxycarbonylation (MO) process. This simulation is based on state of the art Versalis technology using patent data ([40–43]). A box diagram of the process is shown in Fig. 3.

First, methanol, CO and $O_2$ react in the oxycarbonylation reactor to form DMC and water (Eq. (12)) at 24 bar and 130 °C [44]. Due to catalyst deactivation problems derived from the concentration of water in the reactor, the main reaction conversion per pass is limited below 20 % [5]. As such, methanol conversion per pass is fixed of 17 % (99.86 % global conversion) and a selectivity of 97 % towards DMC [41]:

$$2CH_3OH + CO + 1/2O_2 \rightleftarrows (CH_3O)_2CO\ (dimethyl\ \ carbonate) + H_2O \tag{12}$$

The addition of HCl prevents the copper chloride catalyst to lose activity due to the loss of chlorine throughout the reactions [40]. Along with the main DMC formation, secondary reactions such as CO oxidation, DMC hydrolysis, methyl chloride formation and methanol dehydration take place:

$$CO + 1/2O_2 \rightleftarrows CO_2 \tag{13}$$

$$(CH_3O)_2CO + H_2O \rightleftarrows 2CH_3OH + CO_2 \tag{14}$$

$$CH_3OH + HCl \rightleftarrows CH_3Cl\ (methyl\ \ chloride) + H_2O \tag{15}$$

$$2CH_3OH \rightleftarrows (CH_3O)_2O\ (dimethyl\ \ ether) + H_2O \tag{16}$$

Carbon monoxide oxidation (Eq. (13)) is the most relevant of these reactions. Oxygen conversion surpasses 99 % while its selectivity to DMC is known to be greater than 60 % [45]. The rest of the reactions (Eqs. (14)–(16)) are reported to be of small importance since methanol selectivity in the main synthesis is over 95 % [40,46]. As such, the conversions of these reactions are fixed to 0.15 %.

After the reaction, the reactor outlet enters a flash separator, which splits the stream in two. The first one mainly comprises incondensable gases (CO, $CO_2$, $O_2$) while the second includes the product DMC, methanol, water and HCl. Most of the byproducts (methyl chloride, dimethyl ether (DME)) are removed with the gaseous stream. The gases are then cooled down and compressed and the new condensate is recycled back to the original flash unit. The stream (mostly comprised of CO) is recycled back to the reactor, while a small fraction (3.7 %) is purged and burned to produce energy. The combustion of methyl chloride is assumed to follow Eq. (17) [47] and the produced HCl is recov-

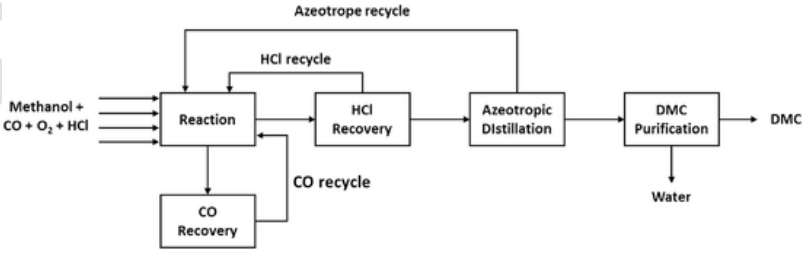


**Fig. 3.** Methanol oxycarbonylation DMC synthesis diagram.

ered:

$$CH_3Cl + 3/2O_2 \rightarrow CO_2 + H_2O + HCl \quad (17)$$

Then, the HCl in the flash liquid effluent is removed in C1 as bottom product (Fig. 4). The overhead product, that contains MeOH, DMC and Water is fed to the azeotropic column C2. This column distills a mixture of MeOH-DMC from the top close to the azeotrope composition, which is then recycled back to the reaction section. The bottom product is a mixture of DMC-Water containing traces of MeOH. This mixture presents a liquid-liquid equilibrium. Therefore, a natural liquid-liquid separation into an organic and aqueous phase will occur in the decanter. The organic phase, rich in DMC, flows to the DMC recovery column, C3, where high purity DMC is recovered as bottom product. On the other hand, the aqueous phase is diverted to the wastewater recovery column, C4. Here, the water in the aqueous phase is obtained as bottom product. The top product of C3 and C4 is a mixture close to the DMC-water azeotrope. These streams are mixed and sent back to the phase separator. (Table 5)

From the results of the simulation, inlet ($F_{j,in}^{DMC}$) and outlet ($F_{j,out}^{DMC}$) molar flows (kmol/s) of the MO process can be calculated using the following mass balances (Eqs. (18)–(24)):

$$F_{CO,in}^{DMC} = 0.90F_{MeOH,in}^{DMC} \quad (18)$$

$$F_{CO,in}^{DMC} = 1.34F_{O_2,in}^{DMC} \quad (19)$$

$$F_{DMC} = 1.08F_{CO,in}^{DMC} \quad (20)$$

$$F_{CO,offgas}^{DMC} = 0.253F_{CO,in}^{DMC} \quad (21)$$

$$F_{CO_2,offgas}^{DMC} = 0.206F_{CO,in}^{DMC} \quad (22)$$

$$F_{H_2,offgas}^{DMC} = F_{H_2,in}^{DMC} \quad (23)$$

$$F_{CH_4,offgas}^{DMC} = F_{CH_4,in}^{DMC} \quad (24)$$

Electricity consumption ($power^{DMC}$, kW) is accounted for using Eq. (25):

$$power^{DMC} = 54.00F_{CO,in}^{DMC} \quad (25)$$

Costs and emission calculations are equivalent to those of the methanol synthesis section (Section 2.3).

### 2.4. Heat integration

Industrial processes that involve syngas production include streams with drastic changes of temperature. The need of heating up a process stream to almost 1000 °C for the reforming step and then cool it down to close to ambient temperature in order to begin with the composition adjustment has associated an important utility consumption. In order to alleviate this energy demand, heat integration can be applied to a process to take advantage of this situation. High temperature streams that need to be cooled down (hot streams) can preheat low temperature streams that require heating (cold streams) and vice versa. We use the transshipment model [48] for this task. This methodology has the advantage of allowing simultaneous heat integration and unit selection in a single optimization due to the model linearity. Furthermore, this approach holds the ability of including several different utilities and limiting the exchange between streams if necessary. On the other hand, it has the downside of not providing the optimal heat exchanger network and thus, being unable to calculate the capital cost of the additional equipment. However, in syngas synthesis related processes, operating costs are much more important than capital costs in the TAC calculation due to the elevated raw material and utility consumption, hence, missing these exchangers barely has an impact on the optimal solutions.

This model considers all hot and cold utility stream requirements for each process unit (furnaces, reformer and regular reactors, heat exchangers, separation columns) in each main section of the superstructure: syngas synthesis, RWGS reactors, methanol synthesis and DMC production. The model comprises 25 hot streams ($h$) and 27 cold streams ($c$) (Table 7) in 69 fin. l stages ($st$). The minimum difference in temperature ($\Delta T_{st}$) for an exchange between to streams to be feasibly carried out is fixed at 10 °C. The equations that define the model are shown below (Eqs. (26)–(28)):

$$\sum_{HS^{s,h}} \left(\Delta T_1 FCp_{st,h} F_{s,j'}^{in}\right) + Q_{hot} = \sum_{CSYN^{s,c}} \left(\Delta T_1 FCp_{st,c} F_{s,j'}^{in}\right) + R_1 \quad \forall j' \in J \quad (26)$$

$$\sum_{HS^{s,h}} \left(\Delta T_{st} FCp_{st,h} F_{s,j'}^{in}\right) + R_{st-1} = \sum_{CSYN^{s,c}} \left(\Delta T_{st} FCp_{st,c} F_{s,j'}^{in}\right) + R_{st} \quad \forall j' \in J,\ \forall st \in ST \setminus \{1, |ST|\} \quad (27)$$

$$\sum_{HS^{s,h}} \left(\Delta T_{|ST|} FCp_{|ST|,h} F_{s,j'}^{in}\right) + R_{|ST|-1} = \sum_{CSYN^{s,c}} \left(\Delta T_{|ST|} FCp_{|ST|,c} F_{s,j'}^{in}\right) \cdot \quad \forall j' \in J$$

where $Q_{hot}$ and $Q_{cold}$ are the total hot and cold utility system requirements in kW, $R_{st}$ is the residual heat (kW) that connects stage $st$ with stage $st+1$, $FCp_{st,h}$ and $FCp_{st,c}$ are the products of the molar flows and heat capacities per kmol/h of component $j'$ (kW hºC/kmol $j'$) of hot stream $h$ and cold stream $c$ located at stage $st$ (Table 7) and $F_{s,j'}^{in}$ is the molar flow of key component $j'$ entering section $s$ ($CH_4$ for syngas production, $CO_2$ for the RWGS reactor and CO for the methanol and DMC sections). The relation sets linking hot ($HS^{s,h}$) and cold ($CS^{s,h}$) streams

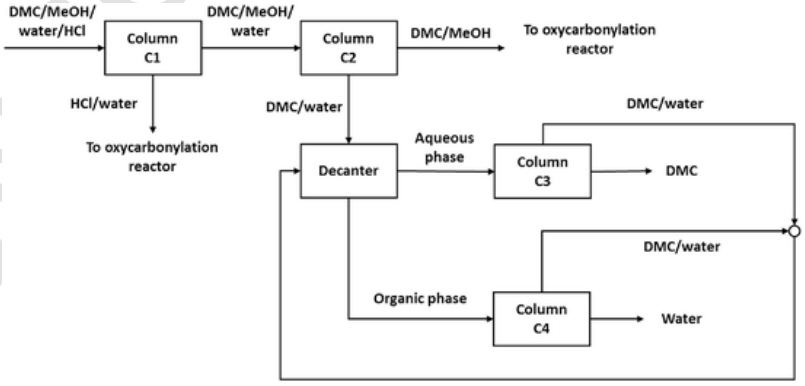


**Fig. 4.** Azeotropic distillation and DMC purification section.

**Table 5**
Column specifications in the DMC purification section (Fig. 4). Temperatures and duties are shown as distillate - bottoms.

| Column | Bottoms recovery | Pressure [bar] | Temperature [ºC] | Duty [kW] | Stages |
|---|---|---|---|---|---|
| C1 | HCl (100 %) | 2.4 | 91.7 – 131.2 | 0 – 8109 | 18 |
| C2 | $H_2O$ (98.96 %) DMC (48.31 %) | 1.5 | 66.4 – 95.5 | 19,478 – 11,351 | 54 |
| C3 | DMC (83.16 %) | 1.2 | 84.3 – 97.4 | 0 – 650 | 12 |
| C4 | $H_2O$ (97.63 %) | 1.2 | 78.8 – 106.2 | 0 – 260 | 12 |

with their respective sections are defined in the nomenclature (indices) section.

Associated cost ($cost^{util}$) and emission ($emission^{util}$) of hot and cold utility consumption are defined using Eqs. (29) and (30):

$$cost^{util} = cost_{hot}\left(Q_{hot} - Q_{hot}^{offgas}\right) + cost_{cold}Q_{cold} \quad (29)$$

$$emission^{util} = GWP_{hot}\left(Q_{hot} - Q_{hot}^{offgas}\right) + 44\sum_{j} G_j F_j^{offgas} \quad (30)$$

Where $Q_{hot}^{offgas}$ (kW) is the energy supplied to the system by burning the off-gas and surplus hydrogen as a fuel calculated as the product of each component $i$ molar flow ($F_i^{offgas}$, kmol/s) and their respective enthalpy of combustion ($\Delta H_j^c$) with an 80 % combustion efficiency, $cost_{hot}$ and $cost_{cold}$ are the costs of acquiring hot and cold utilities (9.2 $/MWh and 1.3 $/MWh, respectively [49]), $GWP_{hot}$ is the associated GWP indicator of burning natural gas (0.212 kg $CO_2$-eq/kWh) and $G_j$ is the number of $CO_2$ moles per mole of combusted component $i$ (Table 6).

## 3. Results and discussion

### 3.1. Simulation of the methanol oxycarbonylation process

The emission and cost results calculated from the proposed methanol oxycarbonylation flowsheet are shown in Table 8. The obtained cost (0.485 $/kg DMC) is below the usual selling price (0.830 $/kg DMC) [50] while the emission (3.301 kg $CO_2$-eq/kg DMC) closely resembles the GWP indicator reported by Garcia-Herrero et al. (3.2 kg $CO_2$-eq/kg DMC) [11]. Both variables are mainly affected by the overall raw material consumption, especially methanol for the cost and CO for the emission. Furthermore, utility consumption also plays and important role in the emission (hot utilities) and the cost (electricity).

The calculated emission value (3.301 kg$CO_2$-eq/kg DMC) of the MO process is, however, a 32.3 % higher than the GWP indicator of the transesterification of ethylene carbonate (2.2347 kg$CO_2$-eq/kg DMC [20]). It is clear that $CO_2$ utilization in the EC route manages to appreciably reduce the GWP indicator of the process, which is unsurprising given the popularity of the technology. However, the potential of the MO route remains untapped. According to the results, reducing the emission related to raw materials should drastically affect the net GWP of the process.

**Table 6**
Combustion enthalpies and molar production of $CO_2$ of the most prominent fuel gas components in the system.

| | $H_2$ | $CH_4$ | CO | $CO_2$ |
|---|---|---|---|---|
| **$\Delta Hc_j$ [kJ/kmol]** | 241,814 | 802,518 | 283,200 | – |
| **$G_j$ [kmol $CO_2$/kmol $j$]** | – | 1 | 1 | 1 |

**Table 7**
Stream information for the transshipment problem.

| Stream | $T_{in}$ [ºC] | $T_{out}$ [ºC] | $FC_p$ [kW hºC·kmol$^{-1}$] |
|---|---|---|---|
| h1 | 900 | 40 | 216 |
| h2 | 1197 | 40 | 99.5 |
| h3 | 1231 | 40 | 171 |
| h4 | 830.7 | 830.6 | 885 |
| h5 | 830.7 | 40 | 196 |
| h6 | 850 | 40 | 129 |
| h7 | 850 | 40 | 193 |
| h8 | 827 | 40 | 271 |
| h9 | 827 | 826.9 | 237 |
| h10 | 300 | 40 | 238 |
| h11 | 350 | 40 | 238 |
| h12 | 400 | 40 | 238 |
| h13 | 450 | 40 | 238 |
| h14 | 48.5 | 40 | 0.09 |
| h15 | 284.3 | 284.2 | 946 |
| h16 | 279.8 | 40 | 0.27 |
| h17 | 123.9 | 53.6 | 0.19 |
| h18 | 140.7 | 67.9 | 0.19 |
| h19 | 134.1 | 134 | 4538 |
| h20 | 39.7 | 20 | 3.07 |
| h21 | 134 | 40 | 6.70 |
| h22 | 139.5 | 115 | 2.53 |
| h23 | 95.5 | 30 | 0.44 |
| h24 | 84.4 | 80.2 | 0.08 |
| h25 | 66.5 | 66.4 | 31,815 |
| c1 | 167.6 | 900 | 265 |
| c2 | 899.9 | 900 | 1970 |
| c3 | 213.9 | 800 | 62.2 |
| c4 | 151.7 | 750 | 160 |
| c5 | 171.4 | 850 | 230 |
| c6 | 849.9 | 850 | 1570 |
| c7 | 40 | 850 | 74.5 |
| c8 | 849.9 | 850 | 2460 |
| c9 | 211 | 850 | 138 |
| c10 | 849.9 | 850 | 2.2 |
| c11 | 142.8 | 827 | 282 |
| c12 | 40 | 300 | 249 |
| c13 | 299.9 | 300 | 45.8 |
| c14 | 40 | 350 | 248 |
| c15 | 349.9 | 350 | 176 |
| c16 | 40 | 400 | 247 |
| c17 | 399.9 | 400 | 300 |
| c18 | 40 | 450 | 248 |
| c19 | 449.9 | 450 | 328 |
| c20 | 139.8 | 284.2 | 0.29 |
| c21 | 68.2 | 134 | 4.88 |
| c22 | 30.6 | 70 | 1.05 |
| c23 | 41.8 | 134 | 0.80 |
| c24 | 131.1 | 131.2 | 13,245 |
| c25 | 95.3 | 95.5 | 18,539 |
| c26 | 106.1 | 97.4 | 1062 |
| c27 | 106.1 | 106.2 | 425 |

### 3.2. Integration of $CO_2$ consumption in the methanol oxycarbonylation process

In this section, carbon monoxide, syngas and methanol production are integrated into the DMC synthesis process. Furthermore, heat inte-

**Table 8**
Emission and cost related to raw materials and energy consumption in the production of DMC by the methanol oxycarbonylation process.

| | | Emission [kg $CO_2$-eq/h] | Cost [$/h] |
|---|---|---|---|
| **Raw materials** | **Mass flow [kg/h]** | | |
| Methanol | 5222 | 3338 | 1567 |
| $O_2$ | 1774 | 2237 | 82.43 |
| CO | 4159 | 7731 | 831.7 |
| HCl | 73.00 | 22.83 | 222.0 |
| Purge* | 3022 | 3022 | – |
| **Utilities** | **Energy [MW]** | | |
| Hot services | 26.21 | 5561 | 242.1 |
| Cold services | 7.139 | – | 9.280 |
| Electricity | 4.236 | 1895 | 552.8 |
| | **Production [kg/h]** | **Emission [kg $CO_2$-eq/kg]** | **Cost [$/kg]** |
| **Total** | **7212** | **3.301** | **0.485** |

* Assumed to suffer a complete combustion.

gration is considered in order to take advantage of the high temperatures achieved in syngas synthesis. Results are divided in four case studies. The base case study considers syngas synthesis without the use of any unconventional technology. The second and third case studies introduce the possibility of selecting the fuel cell and RWGS reactor, respectively. Finally, the fourth case study considers all possible combinations contained in the superstructure. Results are shown in Fig. 5.

The base case scenario illustrates that the usage of Auto-thermal Reforming (ATR) for syngas generation, as well as absorption in the CO separation step, overall achieving the minimum cost for the synthesis of DMC (0.223 $/kg). ATR is one of the most used syngas reforming processes in industry [31], so it is only natural that the minimum cost of the full DMC synthesis contains this technology in its configuration. Furthermore, this cost is reduced over a 50 % in comparison with the non process integration result. The integration of raw material synthesis with the DMC production process removes the need for purchasing both CO and methanol, which naturally avoids a huge percentage of the cost of acquiring the raw materials. Moreover, heat integration vastly reduces hot services, which translates not only in a further decrease in cost, but also in the emission.

Partial Oxidation (POX) and Auto-thermal Reforming (ATR) are two heavily exothermic processes. This exothermicity allows these technologies to supply most, if not all of the hot utilities they require to preheat the feed stream to the reforming reactor from a heat integration implementation [1]. Hence, the interaction of these reforming processes with MO and methanol synthesis is beneficial as POX and ATR can exchange heat at full capability and the energy requirements of the whole system drastically drop.

The GWP indicator of the synthesis falls to 1.400 kg $CO_2$-eq/kg, almost a 60 % decrease compared with the unintegrated base case. At this point, the MO process already possesses an associated emission lower than the EC route (2.2347 kg $CO_2$-eq/kg), even if $CO_2$ is yet to be consumed in the process. The minimum emission configuration of the Base Case maintains ATR as the reforming technology but uses PSA for the separation of CO. However, in this configuration, the cost suffers a 25 % increase while the emission barely achieves a 1 % reduction.

In the second case scenario, which is the addition of a fuel cell for excess hydrogen utilization, the configurations of minimum cost and emission remain the same as in the base case. Nevertheless, the usage of the fuel cell manages to further reduce both indicators. The cost reaches a minimum value of 0.211 $/kg associated to an emission of 1.958 kg $CO_2$-eq/kg, which linearly increases up to a cost of 0.222 $/kg and 1.442 kg $CO_2$-eq/kg as the consumption of surplus $H_2$ in the fuel cell decreases. By further reducing the use of the fuel cell the minimum emission configuration (1.327 kg $CO_2$-eq/kg, 0.286 $/kg) is achieved. These results state that the use of a fuel cell positively affects the cost of the synthesis, however, the emission increases the more hydrogen is used in the unit. The main reason is that, unlike in the case of pure CO production, where $H_2$ is purely a byproduct, $H_2$ is needed in the methanol synthesis process and, therefore, higher $H_2$/CO ratio syngas is needed to be produced to supply the process if it is consumed in the fuel cell, which negatively affects the emission of the synthesis.

The third case scenario, inclusion of a RWGS reactor, shows a drastic change in both the full process configurations and objective values. The use of the reactor changes the utilized syngas reforming process to Partial Oxidation (POX) and the used separation technologies are cryogenic distillation, absorption and PSA in order of increasing cost and decreasing emission. The minimum cost result (0.188 $/kg, 1.296 kg

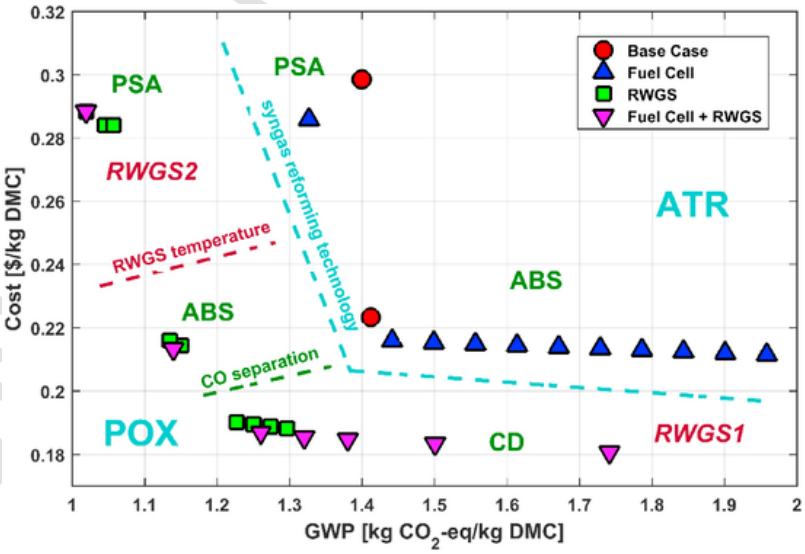


**Fig. 5.** Pareto results of the multi-objective optimization of the integrated CO-syngas-methanol-DMC synthesis. Auto-thermal Reforming, ATR; Partial Oxidation, POX; Pressure Swing Absorption, PSA; Cryogenic Distillation, CD; CO Absorption, ABS; Reverse Water Gas Shift, RWGS. RWGS1 and RWGS2 consider the reaction at 300 and 350 °C with 11.6 and 45 % $CO_2$ conversion, respectively [23]. Clusters of points that use the same technology are indicated with a label nearby. Frontiers (syngas reforming technology, RWGS temperature and CO separation) separate larger groups of points that share some common labels.

$CO_2$-eq/kg) further decreases its value over 10 % in comparison to the fuel cell case scenario. On the other hand, the minimum GWP solution (1.019 kg $CO_2$-eq/kg, 0.288 $/kg) provides the lowest emission achievable by any possible combination contained in the superstructure, offering a 69 % reduction with respect to the unintegrated case and a 54 % in comparison with the $CO_2$ consuming EC route.

The fourth case scenario, inclusion of both a fuel cell and RWGS reactor, results in even lower production costs of DMC (0.181 $/kg, 1.741 kg$CO_2$-eq/kg) that, similarly to the second case scenario, linearly increase while the emission decreases (0.187 $/kg, 1.260 kg$CO_2$-eq/kg) due to the effect of the fuel cell usage. The minimum emission point (1.019 kg $CO_2$-eq/kg, 0.288 $/kg) is shared with the third case scenario, which confirms that the RWGS reactor acts as the most important GWP reduction process unit, while the fuel cell is best used in combination with the RWGS reactor in order to lower the production cost. Furthermore, the RWGS reactor works at a molar $H_2$/CO ratio of seven, 1 bar of pressure and low temperature and $CO_2$ conversion in the minimum cost solutions (300 ˚C, 11.6 %) and requires higher temperature (350 ˚C) and $CO_2$ conversion when minimizing the emission (45 %).

The usage of ATR and POX as the selected syngas reforming technologies can be explained from a material/energy efficiency point of view. The synthesis of DMC from methanol oxycarbonylation requires methanol and CO in a proportion of two to one (Eq. (12)). Methanol, specifically, needs syngas with an $H_2$/CO ratio of approximately two (Eq. (32)) (slightly more due to the simultaneous reaction of $H_2$ and $CO_2$ that yields methanol and water). Globally, this means that DMC requires syngas with an $H_2$/CO ratio of around 4/3, or 1.33.

To analyze the atom efficiency, first, we start with the POX reaction (syngas ratio of two, over the requirements by around 0.67 mol of $H_2$):

$$CH_4 + \frac{1}{2}O_2 \rightarrow 2H_2 + CO \tag{31}$$

We add methanol formation from CO:

$$2H_2 + CO \rightarrow CH_3OH \tag{32}$$

Resulting in:

$$CH_4 + \frac{1}{2}O_2 \rightarrow CH_3OH \tag{33}$$

Then, we add DMC formation (Eq. (12)), which results in:

$$2CH_4 + CO_2 + \frac{3}{2}O_2 \rightarrow CO\left(OCH_3\right)_2 + H_2O \tag{34}$$

Finally, we add the RWGS reaction:

$$H_2 + CO_2 \rightarrow CO + H_2O \tag{35}$$

After following all these steps, we reach the overall reaction from syngas to DMC synthesis:

$$2CH_4 + CO_2 + \frac{3}{2}O_2 + H_2 \rightarrow CO(OCH_3)_2 + 2H_2O \tag{36}$$

In Eq. (36), it can be seen that and additional mole of $H_2$ and half a mole of $O_2$ are included, which produces an additional molecule of water. Even though POX is an important source of energy to the system due to heat integration, atom efficiency is not perfect when adding the RWGS reaction, and an additional mole of $H_2$ needs to be produced, reducing atom efficiency.

Alternatively, we can start this same sequence from the ATR reaction (syngas ratio of 2.5, over the specifications for DMC of around 1.17 mol of $H_2$):

$$CH_4 + \frac{1}{2}O_2 + H_2O \rightarrow 5H_2 + 2CO \tag{37}$$

Following a similar path, we end up with:

$$2CH_4 + CO_2 + O_2 \rightarrow CO(OCH_3)_2 + H_2O \tag{38}$$

Here, the water reaction that was present when POX was considered is missing, which means that the atom efficiency is higher. However, ATR, even if it is also an exothermic reaction, does not reach the same level of heat that the POX reaction achieves due to having to compensate the endothermic simultaneous steam reforming. Even if producing syngas with as much of $H_2$ as possible is usually the goal of reforming, in this particular case, exceeding the ratio is energetically inefficient, since, for one, additional energy is needed to produce this $H_2$ (endothermic steam reforming), and, for two, this $H_2$ is to be transformed back to CO using the RWGS reaction.

However, these two situations, of better atom efficiency but worse energy efficiency, and vice versa, are not numerically too far apart, resulting in a non-intuitive choice at first glance. Due to the results shown in Fig. 5, we can conclude that, even if POX overall reaction when including a RWGS reactor in the superstructure is slightly less materially inefficient the ATR, its exothermicity plays a fundamental role in the energy efficiency of the system, making it the better choice when it is possible to recycle the surplus $H_2$ into CO.

The consumed $CO_2$ versus the GWP indicator of the main results is shown in Fig. 6. The negative consumption found in the base and fuel cell case scenarios is indicative of the net emission of the gas due to the lack of consumption in the selected configurations, since both ATR and POX actually produce the gas. On the other hand, the case scenarios that include the RWGS reactor show a positive consumption, lower when the emission is higher (minimum cost) and peaking when the GWP value is minimum (0.051 kg consumed $CO_2$/kg DMC).

### 3.3. Impact in fuel blend emissions

In order to quantify the potential impact of lowering the production emission of DMC synthesis, we use the obtained GWP results in order to calculate and compare the emissions of DMC –gasoline blends that consist of 5, 10 an 15 %v DMC [10]. In addition, we include MTBE since one of DMC's most important goals in the energy sector is its complete substitution due to the environmental and health problems it carries [10]. The data used in the study is shown in Table 9. Results of this comparison can be seen in Fig. 7.

A striking result of this study is that increasing the quantity of DMC in the gasoline blend, despite improving other properties, rises the overall $CO_2$ emission of its usage (Fig. 7). In contrast, MTBE provides reduced emission blends. The reason of this tendency is the lower heating value (LHV) of DMC (Table 9). While MTBE LHV is slightly lower than gasoline's, DMC LHV is almost three times below, which reduces the volumetric energy of the blend. Hence, emissions are increased per unit of energy when using DMC, but slightly decrease when blending with MTBE.

As the percentage of DMC in the blend rises, so does the emission of the combustion. Since the emission increases linearly, the source of DMC plays a paramount role: the highest the GWP of its production, the steepest the slope, and thus, the fastest the emission increases. This difference gets clearer in mixtures with 15 % DMC, where the $CO_2$ consuming MO presents reductions of approximately 16 and 9 % in comparison with the classic MO and EC routes, respectively.

The contribution of each component of the blend to the overall emission is shown in Fig. 8. Here, it can be seen that the most impactful contribution to the GWP of utilizing the blend is the combustion of gasoline, which is only logical since it is the main component of the mixture. However, the second most important source of emission, at least for the EC and classic MO routes, is the chosen DMC production technology. In the integrated MO case, the combustion and production

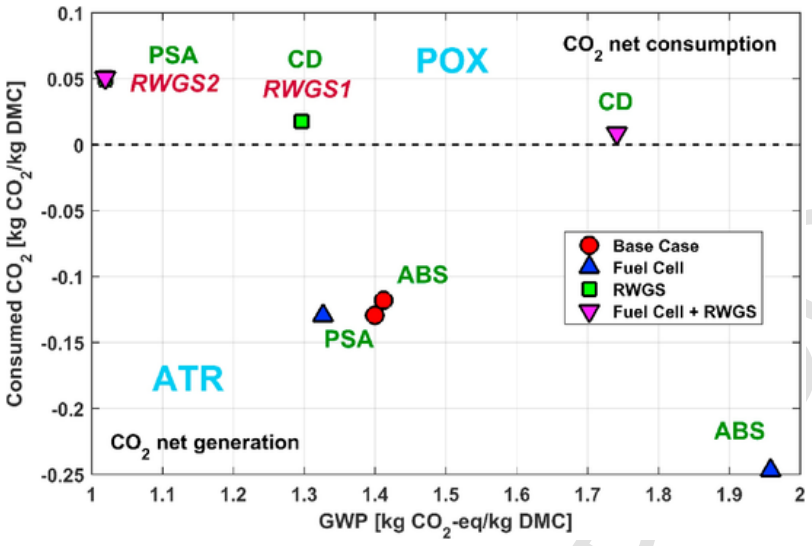


**Fig. 6.** Carbon dioxide consumption of the integrated CO-syngas-methanol-DMC synthesis derived from the results in Fig. 5. Minimum cost and minimum emission results of each case scenario are represented. Auto-thermal Reforming, ATR; Partial Oxidation, POX; Pressure Swing Absorption, PSA; Cryogenic Distillation, CD; CO Absorption, ABS; Reverse Water Gas Shift, RWGS. RWGS1 and RWGS2 consider the reaction at 300 and 350 °C with 11.6 and 45 % $CO_2$ conversion, respectively [23]. Clusters of points that use the same technology are indicated with a label nearby. The horizontal dotted line separates both $CO_2$ consumption/generation and syngas reforming technologies used.

**Table 9**
Gasoline, DMC and MTBE properties [9].

| Compound | Density [kg/m $^3$] | LHV [MJ/kg] | Production GWP [kg $CO_2$-eq/kg] [51] | Combustion emission [kg $CO_2$/MJ] |
|---|---|---|---|---|
| Gasoline | 744.6 | 42.9 | 0.614 | 0.105 [51] ** |
| DMC (Classic MO) | 1070 | 15.8 | 3.301* | 0.092 |
| DMC (Integrated MO) | 1070 | 15.8 | 1.400* | 0.092 |
| DMC ($CO_2$-consuming MO) | 1070 | 15.8 | 1.019* | 0.092 |
| DMC (EC route) | 1070 | 15.8 | 2.235 | 0.092 |
| MTBE | 740.4 | 35.2 | 1.052 | 0.071 |

* This work.
** Includes production (kg $CO_2$-eq/MJ).

emission of DMC are on par, while the GWP reduction of the $CO_2$-consuming MO makes it sufficient to place its contribution to the total emission in the last place, even below than gasoline production GWP. This result, again, states the importance of the additive source GWP. Finally, blends with MTBE present both less emitting production and combustion GWP, which is an effect of its lower LHV.

## 4. Conclusions

Dimethyl carbonate (DMC) is a relevant environmentally friendly compound with many different synthesis routes. Despite including $CO_2$ utilization in its reaction pathway, transesterification of ethylene carbonate (EC) with methanol possesses high Global Warming Potential (GWP). In this work, we propose a process superstructure for the synthesis of DMC using the classic non-$CO_2$ consuming methanol oxycarbonylation technology based on simulations of literature data. Integration of syngas, CO, methanol and DMC production processes manages to drastically reduce both cost (50 %) and emissions (60 %) with respect to the unintegrated synthesis of DMC. The optimal syngas production is carried out using Auto-thermal Reforming (ATR) and Partial Oxidation (POX). The synthesis and utilization of additional hydrogen in a fuel cell further reduce the overall cost. The usage of a Reverse Water Gas Shift (RWGS) reactor as a $CO_2$ sink reduces both cost and emission of the process, especially the latter, which can be as low as 1.019 kg $CO_2$-eq/kg, over a 54 % below than the $CO_2$-consuming EC route (2.2347 kg$CO_2$-eq/kg DMC). The source of DMC when used in gasoline blends appreciably affects the GWP of using the fuel. DMC produced by consuming $CO_2$ in methanol oxycarbonylation potentially achieves reductions of around 16 % in emission in comparison with the direct ethylene carbonate route.

## CRediT authorship contribution statement

**J.D. Medrano-García:** Conceptualization, Methodology, Software, Validation, Investigation, Writing - original draft, Writing - review & editing, Visualization, Funding acquisition. **J. Javaloyes-Antón:** Software, Validation, Investigation, Resources, Writing - review & editing. **D. Vázquez:** Writing - review & editing. **R. Ruiz-Femenia:** Writing - review & editing, Supervision, Funding acquisition. **J.A. Caballero:** Writing - review & editing, Supervision, Funding acquisition.

## Declaration of Competing Interest

The authors declare that they have no known competing financial interests or personal relationships that could have appeared to influence the work reported in this paper.

## Acknowledgments

The authors gratefully acknowledge financial support from the project PROMETEO 2020/064. The authors would also like to thank «Generalitat Valenciana: Conselleria de Educación, Investigación, Cultura y Deporte» for the Ph.D grant (ACIF/2016/ 062).

## Appendix A. Supplementary data

Supplementary material related to this article can be found, in the online version, at doi:https://doi.org/10.1016/j.jcou.2021.101436.

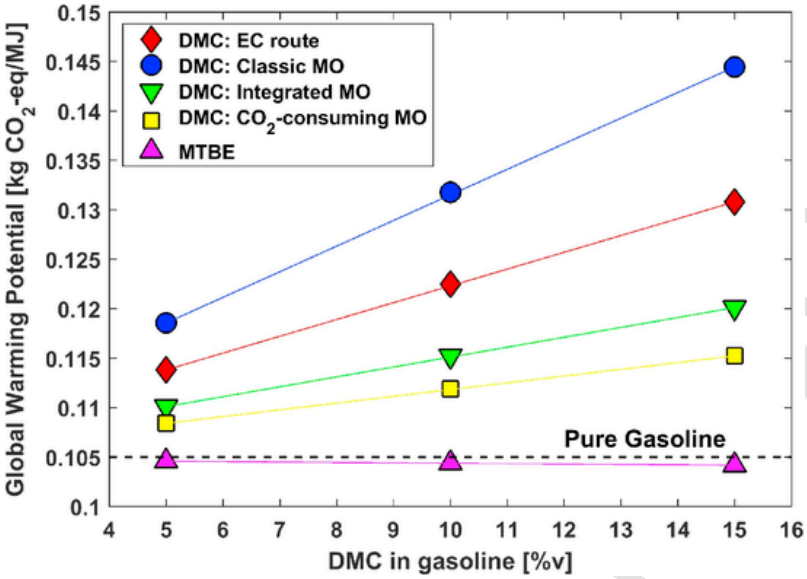


**Fig. 7.** GWP comparison results associated to the use of different source additive-gasoline blends.

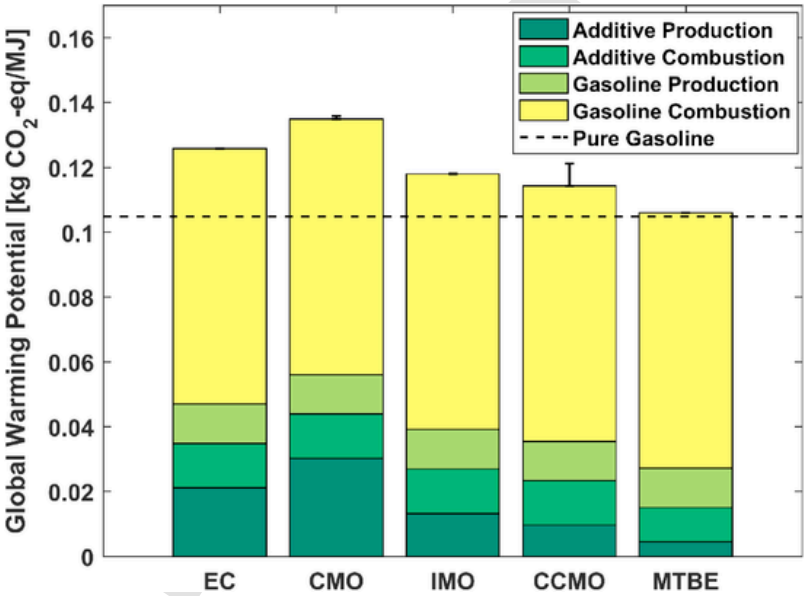


**Fig. 8.** Combustion emission breakdown of the minimum emission configurations of different source 15 % additive-gasoline blends. EC, ethylene carbonate route; CMO, classic methanol oxycarbonylation; IMO, integrated methanol oxycarbonylation; CCMO, $CO_2$-consuming methanol oxycarbonylation; MTBE, methyl tert buthyl ether. Error bars show the maximum emission achievable (minimum cost production).

## References


[1] C. Le Quéré, J.I. Korsbakken, C. Wilson, J. Tosun, R. Andrew, R.J. Andres, J.G. Canadell, A. Jordan, G.P. Peters, D.P. van Vuuren, Drivers of declining CO 2 emissions in 18 developed economies, Nat. Clim. Chang. 9 (2019) 213–217, doi:10.1038/s41558-019-0419-7.

[2] L. Fraccascia, I. Giannoccaro, Analyzing CO2 emissions flows in the world economy using Global Emission Chains and Global Emission Trees, J. Clean. Prod. 234 (2019) 1399–1420, doi:10.1016/j.jclepro.2019.06.297.

[3] P. Friedlingstein, R.M. Andrew, J. Rogelj, G.P. Peters, J.G. Canadell, R. Knutti, G. Luderer, M.R. Raupach, M. Schaeffer, D.P. van Vuuren, C. Le Quéré, Persistent growth of CO2 emissions and implications for reaching climate targets, Nat. Geosci. 7 (2014) 709–715, doi:10.1038/ngeo2248.

[4] C.J. Quarton, S. Samsatli, The value of hydrogen and carbon capture, storage and utilisation in decarbonising energy: insights from integrated value chain optimisation, Appl. Energy 257 (2020) 113936, doi:10.1016/j.apenergy.2019.113936.

[5] M.A. Pacheco, C.L. Marshall, Review of dimethyl carbonate (DMC) manufacture and its characteristics as a fuel additive, Energy Fuels 11 (1997) 2–29, doi:10.1021/ef9600974.

[6] Z. Kricsfalussy, H. Waldmann, H.J. Traenckner, Oxycarbonylation of methanol to dimethyl carbonate using molten salts as catalyst, Ind. Eng. Chem. Res. 37 (1998) 865–866, doi:10.1021/ie9701837.

[7] Z.Z. Yang, L.N. He, J. Gao, A.H. Liu, B. Yu, Carbon dioxide utilization with C-N bond formation: carbon dioxide capture and subsequent conversion, Energy Environ. Sci. 5 (2012) 6602–6639, doi:10.1039/c2ee02774g.

[8] T. Pachiannan, W. Zhong, S. Rajkumar, Z. He, X. Leng, Q. Wang, A literature review of fuel effects on performance and emission characteristics of low-temperature combustion strategies, Appl. Energy 251 (2019) 113380, doi:10.1016/j.apenergy.2019.113380.

[9] A.O.G. Abdalla, D. Liu, Dimethyl carbonate as a promising oxygenated fuel for combustion: a review, Energies 11 (2018) 1–20, doi:10.3390/en11061552.

[10] L. bin Wen, C.Y. Xin, S.C. Yang, The effect of adding dimethyl carbonate (DMC) and ethanol to unleaded gasoline on exhaust emission, Appl. Energy 87 (2010) 115–121, doi:10.1016/j.apenergy.2009.06.005.

[11] I. Garcia-Herrero, R.M. Cuéllar-Franca, V.M. Enríquez-Gutiérrez, M. Alvarez-Guerra, A. Irabien, A. Azapagic, Environmental assessment of dimethyl carbonate production: comparison of a novel electrosynthesis route utilizing CO2 with a

commercial oxidative carbonylation process, ACS Sustain. Chem. Eng. 4 (2016) 2088–2097, doi:10.1021/acssuschemeng.5b01515.
[12] U. Romano, R. Tesel, M.M. Mauri, P. Rebora, Synthesis of dimethyl carbonate from methanol, carbon monoxide, and oxygen catalyzed by copper compounds, Ind. Eng. Chem. Prod. Res. Dev. (1980), doi:10.1021/i360075a021.
[13] N. Keller, G. Rebmann, V. Keller, Catalysts, mechanisms and industrial processes for the dimethylcarbonate synthesis, J. Mol. Catal. A Chem. 317 (2010) 1–18, doi:10.1016/j.molcata.2009.10.027.
[14] W. Peng, N. Zhao, F. Xiao, W. Wei, Y. Sun, Recent progress in phosgene-free methods for synthesis of dimethyl carbonate, Pure Appl. Chem. 84 (2012) 603–620, doi:10.1351/PAC-CON-11-06-02.
[15] R. Chauvy, N. Meunier, D. Thomas, G. De Weireld, Selecting emerging CO2 utilization products for short- to mid-term deployment, Appl. Energy 236 (2019) 662–680, doi:10.1016/j.apenergy.2018.11.096.
[16] K. Shukla, V.C. Srivastava, Synthesis of organic carbonates from alcoholysis of urea: a review, Catal. Rev. - Sci. Eng. 59 (2017) 1–43, doi:10.1080/01614940.2016.1263088.
[17] P. Kumar, V.C. Srivastava, U.L. Štangar, B. Mušič, I.M. Mishra, Y. Meng, Recent progress in dimethyl carbonate synthesis using different feedstock and techniques in the presence of heterogeneous catalysts, Catal. Rev. - Sci. Eng. 00 (2019) 1–59, doi:10.1080/01614940.2019.1696609.
[18] L.F.S. Souza, P.R.R. Ferreira, J.L. de Medeiros, R.M.B. Alves, O.Q.F. Araújo, Production of DMC from CO 2 via indirect route: technical–economical–environmental assessment and analysis, ACS Sustain. Chem. Eng. 2 (2014) 62–69, doi:10.1021/sc400279n.
[19] P. Kongpanna, V. Pavarajarn, R. Gani, S. Assabumrungrat, Techno-economic evaluation of different CO2-based processes for dimethyl carbonate production, Chem. Eng. Res. Des. 93 (2015) 496–510, doi:10.1016/j.cherd.2014.07.013.
[20] Ecoinvent Database 3.5, 2018. https://www.ecoinvent.org/ (accessed May 21, 2019).
[21] R.H. Heyn, Organic Carbonates, Elsevier B.V., 2014, doi:10.1016/B978-0-444-62746-9.00007-4.
[22] S. Rebsdat, D. Mayer, Ethylene oxide, Ullmann's Encycl. Ind. Chem., Wiley-VCH Verlag GmbH & Co. KGaA, Weinheim, Germany, 2001, doi:10.1002/14356007.a10_117.
[23] J.D. Medrano-García, R. Ruiz-Femenia, J.A. Caballero, Optimal carbon dioxide and hydrogen utilization in carbon monoxide production, J. CO2 Util. 34 (2019) 215–230, doi:10.1016/j.jcou.2019.05.005.
[24] S. Lee, I.E. Grossmann, New algorithms for nonlinear generalized disjunctive programming, Comput. Chem. Eng. 24 (2000) 2125–2141, doi:10.1016/S0098-1354(00)00581-0.
[25] M. Ehrgott, M.M. Wiecek, Mutiobjective programming, Mult. Criteria Decis. Anal. State Art Surv., Springer, New York, New York, NY, 2005, pp. 667–708, doi:10.1007/0-387-23081-5_17.
[26] N. Thonemann, M. Pizzol, Consequential life cycle assessment of carbon capture and utilization technologies within the chemical industry, Energy Environ. Sci. 12 (2019) 2253–2263, doi:10.1039/c9ee00914k.
[27] A. Otto, T. Grube, S. Schiebahn, D. Stolten, Closing the loop: captured CO2 as a feedstock in the chemical industry, Energy Environ. Sci. 8 (2015) 3283–3297, doi:10.1039/c5ee02591e.
[28] A. Sánchez, L.M. Gil, M. Martín, Sustainable DMC production from CO2 and renewable ammonia and methanol, J. CO2 Util. 33 (2019) 521–531, doi:10.1016/J.JCOU.2019.08.010.
[29] L. Shi, S.J. Wang, D.S.H. Wong, K. Huang, E.K. Lee, S.S. Jang, Plant-Wide Process Design of Producing Dimethyl Carbonate by Indirect Alcoholysis of Urea, Elsevier Masson SAS, 2018, doi:10.1016/B978-0-444-64241-7.50014-8.
[30] D. Vázquez, J. Javaloyes-Antón, J.D. Medrano-García, R. Ruiz-Femenia, J.A. Caballero, Dimethyl Carbonate Production Process From Urea and Methanol, 2018, pp. 731–736, doi:10.1016/B978-0-444-64235-6.50129-7.
[31] J.D. Medrano-García, R. Ruiz-Femenia, J.A. Caballero, Multi-objective optimization of combined synthesis gas reforming technologies, J. CO2 Util. 22 (2017) 355–373, doi:10.1016/j.jcou.2017.09.019.
[32] A. Nuchitprasittichai, S. Cremaschi, Optimization of CO2 capture process with aqueous amines using response surface methodology, Comput. Chem. Eng. 35 (2011) 1521–1531, doi:10.1016/j.compchemeng.2011.03.016.
[33] K.M.V. Bussche, G.F. Froment, A steady-state kinetic model for methanol synthesis and the water gas shift reaction on a commercial Cu/ZnO/Al2O3Catalyst, J. Catal. 161 (1996) 1–10, doi:10.1006/jcat.1996.0156.
[34] S. Abrol, C.M. Hilton, Modeling, simulation and advanced control of methanol production from variable synthesis gas feed, Comput. Chem. Eng. 40 (2012) 117–131, doi:10.1016/j.compchemeng.2012.02.005.
[35] B. Cañete, C.E. Gigola, N.B. Brignole, Synthesis gas processes for methanol production via $CH_4$ reforming with $CO_2$, $H_2O$, and $O_2$, Ind. Eng. Chem. Res. 53 (2014) 7103–7112, doi:10.1021/ie404425e.
[36] J.D. Medrano, R. Ruiz-Femenia, J.A. Caballero, Multi-objective optimization of a methanol synthesis process superstructure with Two-step carbon dioxide consumption, Comput. Aided Chem. Eng., Elsevier Masson SAS, 2017, pp. 721–726, doi:10.1016/B978-0-444-63965-3.50122-7.
[37] Ecoinvent Database 3.5, 2018. https://www.ecoinvent.org (accessed December 6, 2018).
[38] R. Smith, Chemical Process Design and Integration, 1994, doi:10.1529/biophysj.107.124164.
[39] Eurostat Database, Electricity Prices by Type of User, 2017. https://ec.europa.eu/eurostat/tgm/refreshTableAction.do;jsessionid=W_AzykoJwleWzqhBFk5K4y1LOZivbHBmC4qehHPdshmkD_r5w-W0!1742705336?tab=table&plugin=1&pcode=ten00117&language=en.
[40] F. Rivetti, U. Romano, Procedure for the Production of Alkyl Carbonates, US Patent 5,686,644, 1997.
[41] N. Di Muzio, C. Fusi, F. Rivetti, G. Sasselli, Process for Producing Dimethyl Carbonate, US Patent 5,210,269, 1993.
[42] Eni Versalis, DIMETHYLCARBONATE (DMC) and derivatives based on CO and MeOH ( co-licensing Versalis / Lummus Technology), (n.d.). https://versalis.eni.com/irj/portal/anonymous?guest_user=anon_en&NavigationTarget=ROLES://portal_content/z_eni_ve_fl_versalis/z_eni_ve_fl_roles/z_eni_ve_rl_gues_versalis/LaNostraOfferta/shortcut/Licensing/DMCeDerivati (accessed March 6, 2020).
[43] F. Rivetti, S. Roggero, Procedure for the production of alkyl carbonates, EP 0534545A2, 1992.
[44] D. Delledonne, F. Rivetti, U. Romano, Developments in the production and application of dimethylcarbonate, Appl. Catal. A Gen. 221 (2001) 241–251, doi:10.1016/S0926-860X(01)00796-7.
[45] A. Gami, The DMC / DPC route to polycarbonate feeds: integrated DMC-DPC plant for Green polycarbonate production lummus chemical processes, Versalis Technol. Converence Value to Compete, 2013. http://www.triumphgroupinternational.com/event/wp-content/uploads/sites/15/2013/11/Intermediates-The-DMC-DPC-route-to-Polycarbonate-Feedssmallpdf.com_.pdf.
[46] J. LCLA, B. CMBMB, N. L, R. JR, Catalytic dehydration of methanol to dimethyl ether (DME) using the Al62,2Cu25,3Fe12,5 quasicrystalline alloy, J. Chem. Eng. Process Technol. 04 (2013) 1–8, doi:10.4172/2157-7048.1000164.
[47] A.K. Gupta, Combustion of chlorinated hydrocarbons, Chem. Eng. Commun. 41 (1986) 1–21, doi:10.1080/00986448608911709.
[48] S.A. Papoulias, I.E. Grossmann, A structural optimization approach in process synthesis—II: heat recovery networks, Comput. Chem. Eng. 7 (1983) 707–721, doi:10.1016/0098-1354(83)85023-6.
[49] R. Turton, R.C. Bailie, W.B. Whiting, J.A. Shaeiwitz, D. Bhattacharyya, Analysis, Synthesis and Design of Chemical Processes, fourth, Prentice Hall, 2012.
[50] J. Javaloyes-Antón, D. Vázquez, J.D. Medrano-García, J.A. Caballero, Economic study of the urea alcoholysis process for dimethyl carbonate production, Comput. Aided Chem. Eng., 2019, pp. 61–67, doi:10.1016/B978-0-12-818634-3.50011-4.
[51] G. Wernet, C. Bauer, B. Steubing, J. Reinhard, B. Moreno-Ruiz, E. Weidema, The ecoinvent database version 3 (part I): overview and methodology, Int. J. Life Cycle Assessment, [Online] 21 (9) (2016) 1218–1230. http://link.springer.com/10.1007/s11367-016-1087-8 (accessed January 24, 2020).